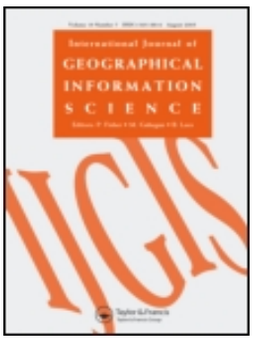

International Journal of Geographical Information Science

ISSN: 1365-8816 (Print) 1362-3087 (Online) Journal homepage: http://www.tandfonline.com/loi/tgis20

Raster modelling of coastal flooding from sea-level rise

B. Poulter & P. N. Halpin

To cite this article: B. Poulter & P. N. Halpin (2008) Raster modelling of coastal flooding from sea-level rise, International Journal of Geographical Information Science, 22:2, 167-182, DOI: 10.1080/13658810701371858

To link to this article: http://dx.doi.org/10.1080/13658810701371858

Published online: 05 Mar 2008.

International Journal of Geographical Information Science
Vol. 22, No. 2, February 2008, 167–182

Taylor & Francis
Taylor & Francis Group

Research Article

Raster modelling of coastal flooding from sea-level rise

B. POULTER*†‡ and P. N. HALPIN†

†Marine Geospatial Ecology Laboratory, Nicholas School of the Environment and Earth Sciences, PO Box 90328, Duke University, Durham, NC 27708, USA

‡Department of Global Change and Natural Systems, Potsdam Institute for Climate Impact Research (PIK), PO Box 60 12 03, D-14412 Potsdam, Germany

(*Received 13 December 2005; in final form 27 March 2007*)

As rates of sea-level rise continue to increase due to climate change, land planners require accurate spatial analyses on the extent and timing of coastal flooding and associated hazards. Digital elevation data used to evaluate coastal vulnerability to flooding are available at various horizontal and vertical resolutions. However, the quality of digital elevation models (DEM) used in environmental assessment can significantly affect the detection of topographic features and the magnitude of hydrological processes. We used lidar elevation data in coastal North Carolina, USA to investigate the effects of horizontal resolution and connectivity on the extent and timing of flooding from sea-level rise. We found that the rate and extent of inundation were dependent on horizontal resolution and assumptions made on hydrological connectivity. The variation in flood extent was much larger (760 km^2) at low sea-level projections (<0.4 m) than at high sea-level projections (>~0.9 m, 114 km^2) due to the effect of hydrological corrections on the coarse-scale DEM and topographic complexity at low elevations. Lidar elevation data provide a significant advance in mapping potential coastal flooding, but the extent and timing of inundation are sensitive to horizontal resolution and the modelling of hydrological connectivity.

Keywords: Sea-level rise; Lidar; Horizontal resolution; Connectivity; Coastal flooding; North Carolina

1. Introduction

Sea level is projected to increase between 0.09 and 0.88 m by the year 2100 due to climate change, thus representing a significant global-scale threat to coastal environments (Church *et al.* 2001, Nichols 2004). While there have been several national and global efforts to map vulnerable coastal regions to sea-level rise (Park *et al.* 1988, Moorhead and Brinson 1995, Blomgren 1999, Nichols 2004, Titus and Richman 2001, Urbanski 2001), the recent availability of high-resolution lidar elevation data for large coastal landscapes has renewed interest in re-evaluating these assessments, as illustrated by the United States Climate Change Science Program Strategic Plan and their report on 'Coastal elevation and sensitivity to sea-level rise'. Currently, there is a need to expand sea-level impact assessments globally as coastal regions become increasingly vulnerable to the effects of sea-level rise and flooding associated with hurricanes (Hecht 2006).

*Corresponding author. Email: ben.poulter@pik-potsdam.de

International Journal of Geographical Information Science
ISSN 1365-8816 print/ISSN 1362-3087 online
http://www.tandf.co.uk/journals
DOI: 10.1080/13658810701371858

Mapping potential sea-level rise impacts is a challenge because the annual sea-level rise increment is about an order of magnitude smaller than the vertical error of most elevation datasets. Consequently, only relatively coarse-scale impact assessments have been conducted due to limitations associated with the vertical resolution of older digital elevation models (1 m or greater). In addition, the framework for modelling inundation from sea-level rise differs to existing flood models that describe short-term, pulsed-flood events. These flood models are dependent on several parameters that include duration of flooding or surface roughness coefficients (Marks and Bates 2000). The long-term inundation resulting from sea-level rise is less dependent on surface roughness features, for example, and research is necessary to expand and improve our understanding on hydraulic characteristics of coastal flooding from sea-level rise.

Digital elevation models derived from lidar provide increased horizontal resolution ($<$20 m grid cell size) compared with previous digital elevation models ($\geqslant$30 m grid cell size). This increased horizontal resolution may improve the accuracy for recognizing topographic features (Lindsay 2006), but at the cost of including redundant elevation data, increasing file size and processing time. These are important trade-offs to consider when determining the horizontal resolution used for analysis, because many hydrology-related processes derived from digital elevation models are scale-dependent (Moore *et al.* 1991, Bolstad and Stowe 1994, Gao 1997, Florinsky and Kuryakova 2000, Holmes *et al.* 2000, Kenward *et al.* 2000, Omer *et al.* 2003, Kienzle 2004) and can affect the delineation of watersheds and channel networks, or floodplain modelling (Wang and Zheng 2005). Increased horizontal resolution may also improve feature recognition for roads or dikes that can have considerable influence over catchment delineation and the spread of flooding. The scale-dependent sensitivity of hydrological processes is especially important for large landscapes where small-scale processes may be important.

Lastly, high-resolution elevation data are appropriate for investigating the influence of topographic complexity on landscape processes. In coastal landscapes, topography is often dissected due to the construction of drainage canals and levees (e.g. the Netherlands, Mississippi delta region, etc.). Due to the narrow and compact organization of drainage channels, they may not always be detected in raster elevation datasets (Duke *et al.* 2003, Lindsay 2006). For example, elevation depressions may falsely appear where levees exist as a result of the interpolation technique and statistical smoothing of point elevations during the creation of a gridded DEM. Consequently, flood models may simulate water moving through these gaps and overestimate flood extent. In regions where data are available, roads and ditches may be used to enforce drainage patterns in a raster elevation model. However, in many regions, these ancillary datasets are not readily available, and researchers must rely on the digital elevation model to accurately represent the surface topography.

Modelling the spread of flooding using raster data can be constrained by specifying whether water flows from one cell to another along only the flat sides of a grid cell (four flow directions, D4), the diagonals or corners of the grid cell, or both (eight flow directions, D8). The selection of a particular connectivity rule (D4 or D8) used for raster-based flood modelling offers a potential solution for enforcing connectivity and constraining flood extent. However, the selection of a connectivity routine may result in significant errors in estimates for land area inundated and/or affect the timing of projected coastal flooding events. Watershed modelling has

well-established algorithms to control water movement across multiple flow directions by proportioning flow between downslope pixels (Tarboton 1997). However, modelling the spread of flooding from sea-level rise is less dependent on these algorithms, as inundation is dependent primarily on elevation.

In this study, we evaluate how the extent and timing of coastal flooding from sea-level rise are affected by horizontal resolution and connectivity. We use lidar elevation data that have recently become available for large coastal landscapes in regions modified by drainage and dike construction. To compare our various inundation models, we evaluated multiple sea-level rise scenarios from the Intergovernmental Panel on Climate Change (IPCC) Third Assessment Report (TAR) ranging up to 1.1 m in 0.025-m increments. This research has global implications for coastal landscapes vulnerable to flooding from sea-level rise, including floodplain mapping in general, especially in regions prone to storm surge associated with hurricanes.

2. Methods

2.1 *Study area*

The study took place in the coastal plain of North Carolina, the location of the second largest estuarine system in the USA, where rates of sea-level rise are among the highest recorded in the world (Douglas and Peltier 2002). North Carolina's coastal plain is located at approximately 35°N and 76°W in the mid-Atlantic region (figure 1). The coastal plain is divided at Cape Lookout by underlying geology into

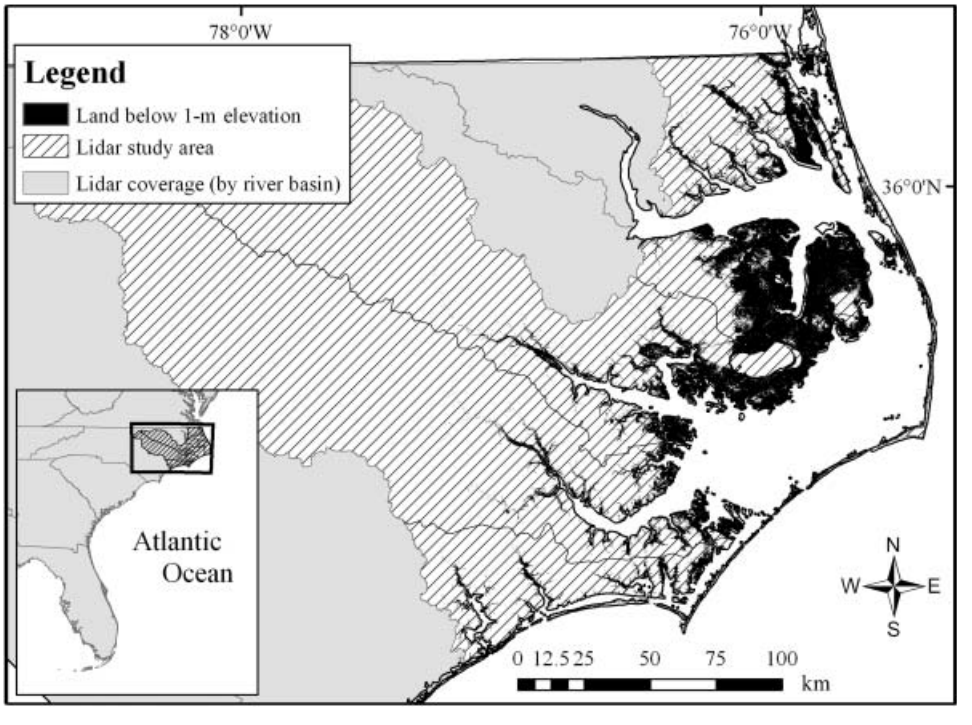

Figure 1. Map of the northern coastal province of North Carolina, USA showing the availability of lidar data acquired in the winter of 2000 and 2001 (http://www.ncfloodmaps.com/status/default.htm) and approximate extent of land below 1-m elevation (NAVD 88).

the Northern and Southern Provinces. Glacial isostatic adjustment is responsible for land subsidence of about 0.2 m per century (Tushingham and Peltier 1991), accounting for the higher than global average rates of local sea-level rise (0.3–0.4 m per century; figure 2). Sea-level is expected to rise between 0.3 and 1.1 m by the year 2100 in response to projected climate change and post-glacial isostatic adjustment (Church *et al.* 2001, Douglas and Peltier 2002).

The marsh and wetland forest ecosystems in our study area are located within the Albemarle-Pamlico Estuarine System, a unique micro-tidal, brackish lagoon with low sediment loads (Wells and Kim 1989, Buzzelli *et al.* 2003). The presence of the barrier islands reduces tidal flux into Albemarle and Pamlico Sounds creating primarily wind-driven tidal conditions (Moorhead and Brinson 1995). Due to these unique environmental conditions, marsh sediment transport models that predict marsh surface elevation to accrete vertically in the presence of a sea-level rise may not be applicable. However, organic accretion in these sediment starved marshes may provide an alternative mechanism for vertical accretion (Craft and Richardson 1998).

Land use is dominated by pine plantations and agricultural fields above an elevation of 0.5 m and is dissected by an extensive network of ditches (up to 3 km ditch km^{-2} of land). The ditch network was originally installed to drain wetlands for agriculture, timber harvest and mosquito control (Lilly 1980). The ditches range in size from narrow agricultural field ditches (~1 m wide) to large canals (~5–7 m wide) connecting side ditches to the estuary. Associated with each ditch are roads or dikes, built from material collected during ditch excavation. The ditch network is thought to have created wetter-than-usual conditions in the interior of the Peninsula, and the ditches are increasingly managed to minimize the impacts of salt intrusion on pine plantations and agriculture.

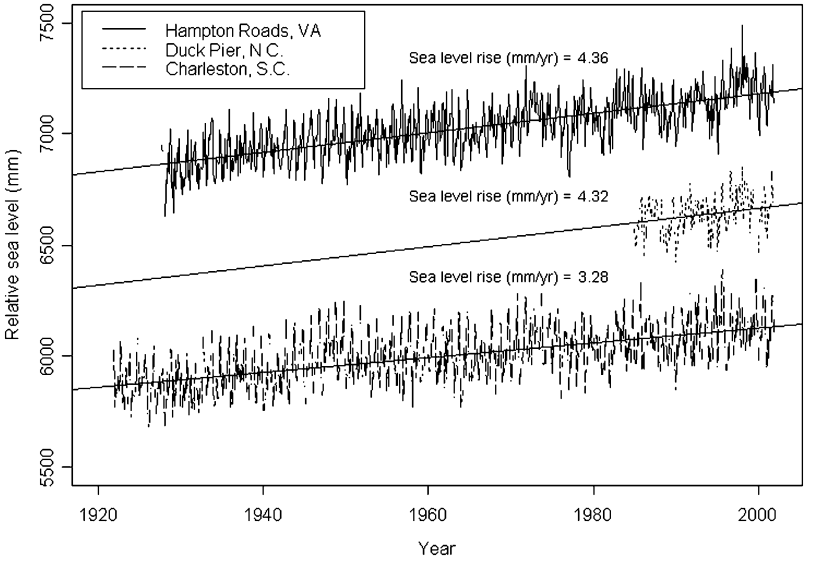

Figure 2. Rates of relative sea-level rise (based on a local benchmark) at Hampton Roads, VA, Duck Pier, NC, and Charleston, SC (PSMSL, 2003).

2.2 *Lidar elevation data*

The North Carolina Floodplain Mapping Program (NCFMP) collected lidar elevation data in the winter of 2000 and 2001 for four major watersheds draining approximately 36 000 km^2 of eastern North Carolina (figure 1). Elevation data were obtained from the NCFMP and merged to create a seamless, sub-metre vertical resolution lidar-based digital elevation model (DEM) for the four watersheds (the Neuse, Pamlico, Pasquotank, and White Oak watersheds) at both 20 and 50 ft horizontal resolution (hereon referred to as 6 and 15 m, respectively). NCFMP hydrologically corrected the 15 m DEM by removing sinks to ensure proper flow direction and by inserting major streams and channels. The enforcement of hydrological flow resulted in a lowering of elevations along streams and channels to maintain the movement of water downslope. Lidar detects only surface features, and as a result, the elevation values for overpasses (built for roads or bridges) were adjusted so that continuous channels were connected either side. The lidar data were projected in stateplane feet (North American Datum 1983), with elevation values referenced to the North American Vertical Datum 1988 (NAVD 88). Approximately 79 km^2 (0.21% of total lidar coverage) of the 15 m DEM were below -5.0 m due to the insertion of artificially low values used as a shoreline breakline by the NCFMP. The elevation values used as a breakline were consequently converted to no data values. The vertical root mean square error ($RMSE_Z$) was calculated separately for the 6 and 15 m DEM using 3480 quality control data points collected and provided by the NCFMP using a Real-Time Kinematic Global Positioning System (RTK-GPS; $RMSE_Z = \pm < 0.01$ m). Following the National Digital Elevation Program and NCFMP (2004) methods we calculated $RMSE_Z$ as:

$$RMSE_Z = \sqrt{\frac{\sum_{i=1}^{n} (z'_i - z_i)^2}{n}} \quad (1)$$

where n is the number of checkpoints, z' is the DEM elevation, z is the quality-control elevation, and i is an integer from 1 to n. The highest 5% of checkpoint errors were discarded to compute the final $RMSE_Z$ following the NC Floodplain Mapping Program procedure to remove sources of random error (NCFMP 2004).

2.3 *Inundation modelling*

Three approaches to modelling hydrological connectivity were developed to simulate inundation of both the 6- and 15-m-resolution lidar DEMs. The first approach was a simple 'bathtub' approach (referred to as a 'zero-side rule') in which a grid cell became flooded if its elevation was less than the projected sea level. The 'zero-side rule' does not consider surface connectivity at all between grid cells and is the approach used in previous studies of sea-level rise (Moorhead and Brinson 1995, Titus and Richman 2001). The second and third approaches specified that the grid cell was flooded only if its elevation was below sea level *and* if it was connected to an adjacent grid cell that was flooded or open water. Two connectivity definitions were used; a 'four-side rule', where the grid cell was connected if any of its cardinal directions were adjacent to a flooded cell, and an 'eight-side rule', where the grid cell was connected if its cardinal and diagonal directions were connected to a flooded grid cell (figure 3, inset). The appropriateness of different connectivity rules is related to our ability to accurately resolve surface flow connections. A 'four-sided'

Figure 3. Modelled inundation for a 25 km^2 subsection of northern Tyrrell County, NC using a 0.10- and 0.125-m rise in sea level illustrating differences in area inundated as a function of grid-cell horizontal resolution (grain size) and connectivity rule. The inset shows the difference between 4-side and 8-side connectivity rules. Currently, a culvert allows water to pass under the road (in the centre of each image).

rule may have the potential to underestimate surface flow connections because only cell sides are allowed to be connected. Conversely, the 'eight-sided' rule may have the potential to overestimate connectivity by allowing flow to occur across cell corners that may overestimate the existence of true surface flow connections. The connectivity rule selected and spatial resolution of the DEM cells act together to influence the accuracy of our depiction of connectivity for different topographic surface features at different spatial scales. The following equation describes how the model was used to predict flooding (F):

$$F_{x,y} = \begin{cases} E_{x,y} \leq S, 1 \\ E_{x,y} > S, 0 \end{cases} \cdot C_i \quad (2)$$

where F is binomial, either flooded (1) or not flooded (0), E is lidar elevation at location x, y, S is projected sea level, C represents connectivity (connected (1) or not connected (0)), and i is an integer specifying the 'bathtub', cardinal, or cardinal and diagonal connectivity rules ('zero-side rule', 'four-side rule', or 'eight-side rule', respectively).

Inland lakes and water bodies were excluded from our analysis due to a lack of information on water surface elevations and potential interactions with sea-level rise. All the land elevations around the main lake in our study (Lake Mattamuskeet) were below 0.12 m and flooded at this sea level. We assumed that below this

elevation, inland areas connected to the lake were not inundated with sea-level rise. We also assumed that the vadose zone (unsaturated soil) and surface roughness did not affect inundation because the time (t) for diffusion was infinity (i.e. the process of sea-level rise overwhelms diffusivity constraints). However, previous work suggests that groundwater tables will move upward as sea level elevates water through the unsaturated zone to the soil surface (Nuttle and Portnoy 1992), although this process is poorly understood at the landscape scale.

The model was initiated with a sea-level value of −0.25 m (to account for inland areas currently below 0 m NAVD 88) and ended at 1.1 m in 0.025-m increments (55 total increments) for the three connectivity rules and two DEM resolutions creating a total of 330 raster flood surfaces. We computed the area inundated with rising sea level for the entire study area and mapped various inundation scenarios to visualize the effects of roads and ditches. The resulting data are presented to assess differences between models on cumulative area of land inundation as well as the rates of land inundated per unit rise in sea level.

3. Results

3.1 *Lidar error*

The lidar $RMSE_Z$ was 0.16 m for the 6-m DEM and 0.20 m for the 15-m DEM with the highest 5% of the checkpoint errors removed (table 1). This is within the range of expected error for lidar datasets and approximately an order of magnitude lower than 7.5-min USGS Level 1 DEMs (Maune 2001) used in previous sea-level-rise assessments. A large area of land in our study area (between 537 and 558 km^2) was below 0-m elevation (relative to NAVD 88; see table 2). According to the North Carolina land cover from the USGS GAP Analysis (McKerrow *et al.* in prep.), 80% of this land cover was open water, cypress-gum swamp, coastal plain non-riverine wet flat forest, agriculture fields, tidal marsh, tidal swamp, pocosin, and coniferous

Table 1. Vertical root mean square error ($RMSE_Z$) for 6-m and 15-m horizontal resolution lidar topographic elevation models.

Digital elevation model	Horizontal resolution (m)	$RMSE_Z$ (m)	$RMSE_Z$ (m; 5% highest checkpoints discarded)
Lidar	6	0.26	0.16
	15	0.40	0.20

Table 2. Model estimates of land area inundated for a 0.3-, 0.5-, 0.8-, and 1.1-m rise in simulated sea level in the northern coastal province of North Carolina.

Projected sea level (m)	Land area inundated (km^2)					
	6-m DEM			15-m DEM		
	0 side-rule	4 side-rule	8 side-rule	0 side-rule	4 side-rule	8 side-rule
0	429	195	206	558	326	542
0.3	1746	1112	1178	1873	1578	1868
0.5	2857	2398	2459	2926	2770	2922
0.8	3970	3746	3797	3984	3896	3981
1.1	4683	4553	4572	4668	4609	4665

plantation, while the remaining area was composed of minor contributions from other plant communities. We verified that the negative elevations were not systematic errors by comparing them with RTK-GPS elevation control points (measured by NCFMP).

3.2 *Effects of horizontal resolution and connectivity on inundated area*

There were large differences in the extent and timing of inundation that were dependent on the horizontal resolution of the DEM and the approach for connectivity modelling. Regardless of which connectivity model was used, the 15-m-resolution DEM predicted greater areas of inundation than the 6-m DEM (table 2). The difference between DEM resolution was greatest at low sea-level-rise projections (<0.3 m) and decreased at high projections (>0.8 m). For example, a 0.3-m rise in sea level inundated a minimum of 1112 km^2 and a maximum of 1873 km^2 of land, a 761-km^2 difference between models (table 2). In contrast, at higher sea-level projections (1.1 m), the variation between inundation estimates converged with 4553 to 4668 km^2 of land inundated, reducing the difference to only 115 km^2 (table 2).

Specifying connectivity (four- or eight-side rule) resulted in lower inundation estimates than the zero-side rule (no connectivity). As expected, the four-side rule reduced the number of connections between flooded cells and decreased the area of the landscape that was flooded. The eight-side rule increased the number of connections (relative to the four-side rule) and consequently, and the area that was flooded increased accordingly. Enforcing hydrological connectivity increased the importance of fine-scale landscape features such as ditches and dikes (figure 3). In the presence of topographic barriers, connectivity forced water to pass around rather than flood low-elevation cells in front of and behind the obstructions. For example, in one location, a dike associated with a road prevented inland inundation only when the four-side rule for connectivity was specified (figure 3). However, at this same location, flooding extended inland with the zero or eight-side rule because the dike was not recognized with the less constrained connectivity assumptions.

The rules for hydrological connectivity interacted strongly with DEM horizontal resolution (figure 3). The extent of flooding modelled with the 6-m DEM was much less than the 15-m DEM when connectivity was specified. For example, the difference in area flooded between the 6- and 15-m DEM with a 0.3-m rise in sea level was 127 km^2 for the zero-side rule, increasing to 466 km^2 and 690 km^2 for the D4 and D8 rules, respectively. Flooding extended further inland with the 15-m DEM along channels resulting from the hydrological correction algorithm applied by NCFMP, but topographic complexity detected in the 6-m DEM also contributed to fragmenting hydrological connectivity.

3.3 *Landscape and county impacts*

The total area of land inundated under the 1.1-m sea-level rise scenario (the high IPCC eustatic sea-level projection including regional isostatic subsidence for the year 2100) for the study area ranged between 4553 and 4683 km^2 (table 2). Inundation for the 6-m DEM lagged behind the 15-m DEM (for all connectivity models) until 0.925 m when the 6-m DEM had a slightly higher area inundated for the zero-side model (figure 4). Compared with other studies, the total area inundated was of a similar order of magnitude (Moorhead and Brinson 1995, Titus and Richman 2001).

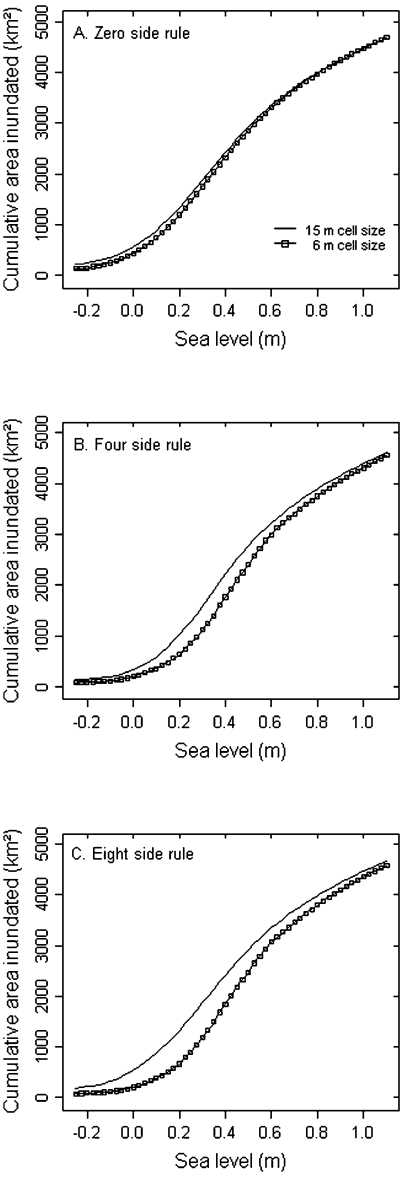

Figure 4. Cumulative land area inundated for the northern coastal province of North Carolina, USA (Figure 1) for each of the six inundation models using 0.025-m sea-level-rise increments up to 1.1 m.

The area inundated showed a nonlinear response to sea-level rise (figure 4) which reflected the distribution of elevations of the outer coastal plain, which has extensive low-relief peat deposits (Poulter *et al.* 2006). The rate of land inundated was higher below 0.4-m elevation, and then decreased above this elevation (figure 5). There was considerable variation in the rate of inundation that was dependent on the horizontal resolution and connectivity approach. The zero-side rule for the 6- and 15-m-horizontal-resolution DEMs showed a gradual increase in the rate of inundation followed by a decrease over the range of sea-level projections.

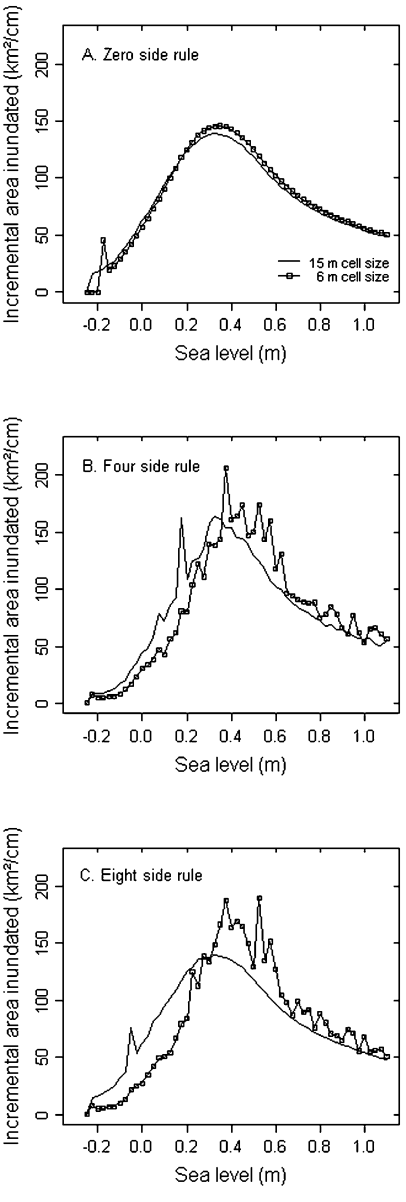

Figure 5. Incremental land area inundated per unit rise in sea level (the rate of land inundated with a unit rise in sea level).

However, the four- and eight-side rules had rates of inundation that were not gradual, but showed abrupt increases and decreases (figure 5). On further investigation, these abrupt changes in inundation rate were related to 'breaching' events of dikes, with each spike or jump in the 'rate' curve representing a large inundation event. These inundation events took place where a large area of land that had been below sea level for several flood increments abruptly became connected to an inundated grid cell. For all six models, the highest rates of inundation occurred while the sea level was below ~0.4 m with rates up to 200 km^2 of land inundated per centimetre rise in sea level.

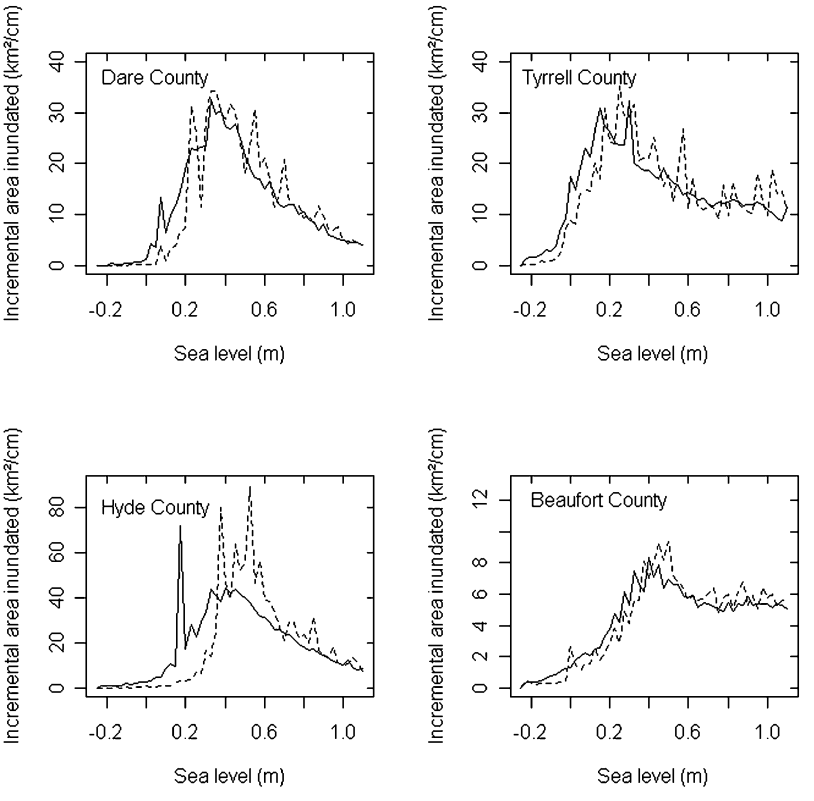

Figure 6. Area inundated (by county) using the 4-side connectivity rule. The solid line represents the 15-m DEM, and the dashed line represents the 6-m DEM. The *y*-axis differs between graphs.

The overall trend in total inundation and rate of inundation remained similar at the county scale to the landscape (figure 6). Depending on the distribution of elevations within a county, the highest rate of inundation was reached at different elevation thresholds. For example, the rate of inundation reached a plateau at 6 and 10 $km^2\,cm^{-1}$ for Beaufort and Tyrrell County (figure 6), respectively, because much of the land in these counties is above 1.1 m. For Hyde and Dare Counties, however, over 70% of the land was inundated, with little land above 1.1 m causing the rates of area inundated to decrease significantly. The timing of breach events was strongly coupled to horizontal resolution, especially for Hyde County, where there was a 0.2-m difference in sea level for the occurrence of a major breach that was dependent on which resolution of the model has used (figure 6).

4. Discussion

4.1 *Capacity of lidar to model sea-level rise impacts*

Previous approaches to modelling inundation from simulated sea-level rise have been limited by coarse-resolution elevation datasets (Park *et al.* 1988, Moorhead and Brinson 1995, Titus and Richman 2001, Nichols 2004). Our study shows that while higher-resolution elevation data represent a significant advance for modelling sea-level rise impacts, there can be a large variability in inundation estimates that

depend on the technique used for interpolation and post-processing of lidar points into a DEM and on the assumptions for maintaining hydrological connectivity. Remote sensing and field-based research will be necessary to assess and validate the various approaches for inundation modelling. However, validation of modelled inundation from sea-level rise is challenged by the long temporal and large spatial scales that characterize this process.

Horizontal resolution was more important at lower sea-level projections and when connectivity was specified than compared with high sea-level projections. For all six scenarios, our analysis resulted in only a 3% difference in the area inundated for a 1.1-m rise in sea level; however, the difference was as high as 65% at the 0.3-m projection. Using the zero-side rule, the difference in area inundated was primarily the result of statistically smoothing elevation values when rescaling from 6- to 15-m spatial resolution. However, when connectivity was specified, two factors influenced the difference in inundation estimates: (1) the primary effects of the hydrological correction algorithm; and (2) the secondary effects of micro-topography.

The removal of topographic 'sinks' and the enforcement of stream and channel networks resulted in a DEM more porous for water movement, as well as lower elevation values along drainage lines. This hydro-correction procedure ensures flow connectivity of surface water, which is critical to floodplain mapping, currently a major use for topographic lidar. When connectivity was not specified, the effect of the hydrological correction on flood extent was minimal at all elevations, and the difference between the 6- and 15-m DEM was small. Specifying connectivity (either the D4 or D8) resulted in inundation closely following the enforced drainage network, resulting in larger areas inundated for the 15-m, hydro-corrected DEM. This was illustrated by the secondary effect of micro-topography, which was important at low elevations for the 6-m DEM as compared with the topographically smoothed 15-m DEM.

At lower sea-level projections (<0.4 m), fine-scale topographic complexity increases partly because the extensive ditch and dike network becomes more important. This increase in topographic complexity at low elevations caused significant disruptions in hydrological connectivity. In contrast, at high sea-level projections (>0.4 m) topographic complexity appeared to decrease, and the estimates of inundation became more similar between DEMs. These differences are evident in figure 7, a cross-section of the 6- and 15-m DEM, illustrating the effects of horizontal resolution on the complexity of the elevation surface. In this figure, fine-scale features such as roads, ditches, dikes, and also the 'hummocky' surface, typical of wetland forests (Bruland and Richardson 2005), are evident at higher horizontal resolutions and, at the landscape scale, contribute significantly to the extent of inundation.

4.2 *Thresholds*

Previous inundation assessments focused on sea-level projections that corresponded to DEM resolution or the closest contour interval to projected sea level (Moorhead and Brinson 1995). These modelling approaches are unable to identify potential thresholds where rates of inundation can change abruptly in response to topographic complexity or in response to changing landscape morphology. As our study demonstrates in North Carolina, various thresholds and patterns in the rates of inundation exist, which can provide valuable information to managers and policymakers anticipating the response of ecosystems to gradual environmental

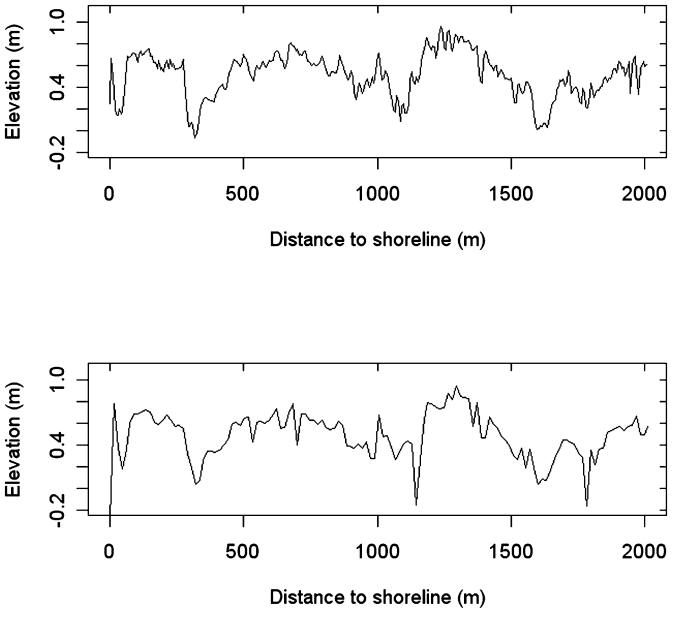

Figure 7. Elevation profile (2-km length) from northern Tyrrell County, North Carolina, USA. The top figure (*a*) is the elevation profile for the 6-m lidar DEM, and the lower figure (*b*) is the same elevation profile using the 15-m lidar DEM.

change. In north-eastern North Carolina, all six-inundation models identified a threshold where the highest rate of inundation was well below 1-m elevation. The highest rate of land inundated (200 km^2 per cm rise) occurred while the sea level was below approximately 0.4 m elevation. At the observed rate of sea-level rise, this projection will be reached by 2100, or sooner if climate change continues to increase the current rate of sea-level rise.

Our study also illustrates that land planners in adjacent counties in North Carolina will observe sea-level impacts at different times, making landscape-scale planning complex. Fortunately, the high horizontal resolution derived from lidar data can assist planning and management responses to sea-level rise by being more site-specific; however, considerable variability still exists depending on lidar post-processing routines and connectivity assumptions. For example, depending on the choice of model, there is a 50-year window of uncertainty for the timing of a dike-overtopping event in Beaufort County (figure 7) with this type of uncertainty common throughout the landscape.

4.3 *Additional uncertainties*

In addition to uncertainties regarding the modelling approach, there are several potential ecological feedbacks and uncertainties that our model does not consider. These include the effects of vertical accretion in marshes and in some wetland forests that could compensate for the effects of sea-level rise. While ground fires and peat oxidation (from the lowering of the water table by ditches) may contribute to local subsidence (Poulter *et al.* 2006), surface elevations may continue to increase in some areas and mitigate inundation. Conversely, shoreline erosion rates in this region are high (Riggs 2001) and may increase with sea-level rise and present an additional

threat to landscape stability. Lastly, discrepancies between the vertical datum used to reference lidar elevation to current sea level (NAVD88) and the location of actual mean sea level (LMSL) present additional errors (± 6 cm) that are significant at the magnitude of predicted sea-level rise. The net result of these processes may act to either mitigate or exacerbate the effects of sea-level rise in this region and need to be considered when coupling physical and biological sea-level rise models.

4.4 *Interactions with floodplain mapping*

This study raises several issues for floodplain mapping in general and for modelling impacts of storm surge events associated with hurricanes and other intense weather phenomena. As sea level continues to rise, floodplain boundaries will shift further inland and upland. Storm surge events from hurricanes may become more severe in response to climate change (Trenberth 2005) and interact with sea-level rise, causing more severe flooding than current flood models predict. For example, dikes currently preventing coastal flooding may be overtopped in the future as sea level rises and storms become more severe. Current mitigation of landscapes for sea-level rise or mapping of floodplain boundaries ought to consider the baseline from which sea level is measured as dynamic and continuously changing in response to climate change.

5. Conclusion

The availability of high-resolution lidar elevation data for large coastal landscapes provides an opportunity to re-evaluate previous sea-level rise impact studies. This study suggests that in coastal North Carolina, lidar post-processing, horizontal resolution, and connectivity rules can produce significantly different outcomes in inundation estimates. In many coastal landscapes, topographic complexity is enhanced by the presence of ditches and dikes, features difficult to detect, even with high-spatial-resolution DEMs (Lindsay 2006). Selecting appropriate connectivity rules or horizontal resolution may minimize errors resulting from absent fine-scale features; however, when road and ditch data are available, enforcing the presence of dikes or ditches through the use of raster-based algorithms may be preferable (Duke *et al.* 2003).

DEMs derived from lidar elevation data provide an additional benefit by allowing multiple, or transient, sea-level-rise scenarios to be evaluated. In North Carolina, our study identified an important threshold effect where the impacts of sea-level rise are greatest in the short term (or below 0.4 m) and then gradually decrease, which previous coarse-scale analyses were unable to detect. Nonlinear sea-level inundation impacts may exist in other low-lying or deltaic landscapes where sea-level rise poses a significant problem and will be important to recognize for mitigation and adaptation strategies. The modelling framework presented in this paper illustrates that land planners and managers mitigating the extent of coastal inundation must consider variability from model selection and hydrological assumptions.

Acknowledgements
Additional comments by Dr N. L. Christensen, Dr J. M. Varner III, and three anonymous reviewers improved the quality of this manuscript. This work was supported by NASA Headquarters under the Earth System Science Fellowship Grant NGT5-30472.

References

BLOMGREN, S., 1999, A digital elevation model for estimating flooding scenarios at the Falsterbo Peninsula. *Environmental Modelling and Software*, **14**, pp. 579–587.

BOLSTAD, P.V. and STOWE, T., 1994, An evaluation of DEM accuracy: Elevation, slope and aspect. *Photogrammetric Engineering and Remote Sensing*, **60**, pp. 1327–1332.

BRULAND, G.L. and RICHARDSON, C.J., 2005, Hydrologic, edaphic, and vegetative responses to microtopographic reestablishment in a restored wetland. *Restoration Ecology*, **13**, pp. 515–523.

BUZZELLI, C.P., RAMUS, J.R. and PAERL, H.W., 2003, Ferry-based monitoring of surface water quality in North Carolina estuaries. *Estuaries*, **26**, pp. 975–984.

CAHOON, D.R., DAY, J.W., Jr., REED, D.J. and YOUNG, R.S., 1998, Global climate change and sea-level rise: estimating the potential for submergence of coastal wetlands. In *Vulnerability of Coastal Wetlands in the Southeastern United States: Climate Change Research Results*, G.R. Guntenspergen and B.A. Varin (Eds), pp. 21–35 (Washington, DC: USA, USGS, Biological Resources Division, Biological Science Report).

CHURCH, J.A., GREGORY, J.M. and HUYBRECHTS, P., et al. 2001, Changes in sea level. In *Climate Change 2001: The Scientific Basis*, J.T. Houghton, Y. Ding, D.J. Griggs, M. Noguer, P. van der Linden and D. Xiaosu (Eds), pp. 639–693 (Cambridge: Cambridge University Press, Contribution of Working Group I to the Third Assessment Report of the Intergovernmental Panel on Climate Change).

CRAFT, C.B. and RICHARDSON, C.J., 1998, Recent and long-term organic soil accretion and nutrient accumulation in the everglades. *Soil Science Society of America Journal*, **62**, pp. 834–843.

DOUGLAS, B.C. and PELTIER, W.R., 2002, The puzzle of global sea level rise. *Physics Today*, **55**, pp. 35–40.

DUKE, G.D., KIENZLE, S.W., JOHNSON, D.L. and BYRNE, J.M., 2003, Improving overland flow routing by incorporating ancillary road data into digital elevation models. *Journal of Spatial Hydrology*, **3**, pp. 1–27.

FLORINSKY, I.V. and KURYAKOVA, G.A., 2000, Determination of grid size for digital terrain modelling in landscape investigations—exemplified by soil moisture distribution at a micro-scale. *International Journal of Geographical Information Science*, **14**, pp. 815–832.

GAO, J., 1997, Resolution and accuracy of terrain representation by grid DEMs at a micro-scale. *International Journal of Geographical Information Science*, **11**, pp. 199–212.

HECHT, J., 2006, Disappearing deltas could spell disaster. *New Scientist*, **189**, pp. 8–11.

HOLMES, K.W., CHADWICK, O.A. and KYRIAKIDIS, P.C., 2000, Error in a USGS 30-meter digital elevation model and its impact on terrain modeling. *Journal of Hydrology*, **233**, pp. 154–173.

KENWARD, T., LETTENMAIER, D.P., WOOD, E.F. and FIELDING, E., 2000, Effects of digital elevation model accuracy on hydrologic predictions. *Remote Sensing of Environment*, **74**, pp. 432–444.

KIENZLE, S., 2004, The effect of DEM raster resolution on first order, second order and compound terrain derivatives. *Transactions in GIS*, **8**, pp. 83–111.

LILLY, J.P., 1980, A history of land development in North Carolina. In *Pocosin Wetlands*, C.J. Richardson, (Ed), pp. 20–39 (Stroudsburg, PA: Hutchinson Ross).

LINDSAY, J.B., 2006, Sensitivity of channel mapping techniques to uncertainty in digital elevation data. *International Journal of Geographical Information Sciences*, **20**, pp. 669–692.

MCKERROW, A.J., WILLIAMS, S.G. and COLLAZO, J.A., 2006, *The North Carolina Gap Analysis Project: Final Report* (Raleigh, NC: North Carolina Cooperative Fish and Wildlife Research Unit). Submitted to the National Gap Analysis Program, U.S. Geological survey, Biological Resources Discipline.

MARKS, K. and BATES, P., 2000, Integration of high-resolution topographic data with floodplain flow models. *Hydrological Processes*, **14**, pp. 2109–2122.

MAUNE, D.F., 2001, *Digital Elevation Model Technologies and Applications: The DEM User's Manual* (Bethesda, MD: American Society for Photogrammetry and Remote Sensing).

MOORE, I.D., GRAYSON, R.B. and LADSON, A.R., 1991, Digital terrain modeling: A review of hydrological, geomorphological, and biological applications. *Hydrological Processes*, **5**, pp. 3–30.

MOORHEAD, K.K. and BRINSON, M.M., 1995, Response of wetlands to rising sea level in the lower coastal plain of North Carolina. *Ecological Applications*, **5**, pp. 261–271.

MORRIS, J.T., SUNDARESHWAR, P.V., NIETCH, C.T., KJERFVE, B. and CAHOON, D.R., 2002, Responses of coastal wetlands to rising sea level. *Ecology*, **83**, pp. 2869–2877.

NCFMP, 2004, *Issue 37: Quality Control of Light Detection and Ranging Elevation Data in North Carolina for Phase II of the North Carolina Floodplain Mapping Program* (Raleigh, North Carolina: North Carolina Cooperating Technical State Mapping Program).

NICHOLS, R.J., 2004, Coastal flooding and wetland loss in the 21st century: changes under the SRES climate and socio-economic scenarios. *Global Environmental Change*, **14**, pp. 69–86.

NUTTLE, W.K. and PORTNOY, J.W., 1992, Effects of rising sea level on runoff and groundwater discharge to coastal ecosystems. *Estuarine, Coastal, and Shelf Science*, **34**, pp. 203–212.

OMER, C.R., NELSON, E.J. and ZUNDEL, A.K., 2003, Impact of varied data resolution on hydraulic modeling and flood plain delineation. *Journal of the American Water Resources Association*, **39**, pp. 467–475.

PARK, R.A., TREHAN, M.S., MAUSEL, P.W. and HOWE, R.C., 1988, *The Effects of Sea Level Rise on U.S. Coastal Wetlands* (Indianapolis, IN: Holcomb Research Institute, Butler University).

POULTER, B., CHRISTENSEN, N.L. and HALPIN, P.N., 2006, Carbon emissions from a temperate peat fire and its relevance to interannual variability of trace atmospheric greenhouse gases. *Journal of Geophysical Research*, **111**, doi:10.1029/2005JD006455.

PSMSL, 2003, *Sea Level Records* (Permanent Service for Mean Sea Level). Available online at: http://www.pol.ac.uk/psmsl/ (accessed 1st February 2003).

RIGGS, S.R., 2001, *Shoreline Erosion in North Carolina's Estuaries* (Raleigh, NC: North Carolina Sea Grant Program, North Carolina State University).

TARBOTON, D.G., 1997, A new method for the determination of flow directions and upslope areas in grid digital elevation models. *Water Resources Research*, **33**, pp. 309–319.

TITUS, J.G. and RICHMAN, C., 2001, Maps of lands vulnerable to sea level rise: modeled elevations along the US Atlantic and Gulf coasts. *Climate Research*, **18**, pp. 205–228.

TRENBERTH, K., 2005, Uncertainty in hurricanes and global warming. *Science*, **308**, pp. 1753–1754.

TUSHINGHAM, A.M. and PELTIER, W.R., 1991, A new global model of late Pleistocene deglaciation based upon geophysical predictions of post glacial relative sea level change. *Journal of Geophysical Research*, **96**, pp. 4497–4523.

URBANSKI, J., 2001, The impact of sea-level rise along the Polish Baltic Coast. *Journal of Coastal Conservation*, **7**, pp. 155–162.

WANG, Y. and ZHENG, Z., 2005, Comparison of light detection and ranging and national elevation dataset digital elevation model on floodplains of North Carolina. *Natural Hazards Review*, **6**, pp. 34–40.

WELLS, J. and KIM, S., 1989, Sedimentation in the Albemarle-Pamlico lagoonal system: synthesis and hypotheses. *Marine Geology*, **88**, pp. 263–284.